SUPPLEMENTARY FIGURES

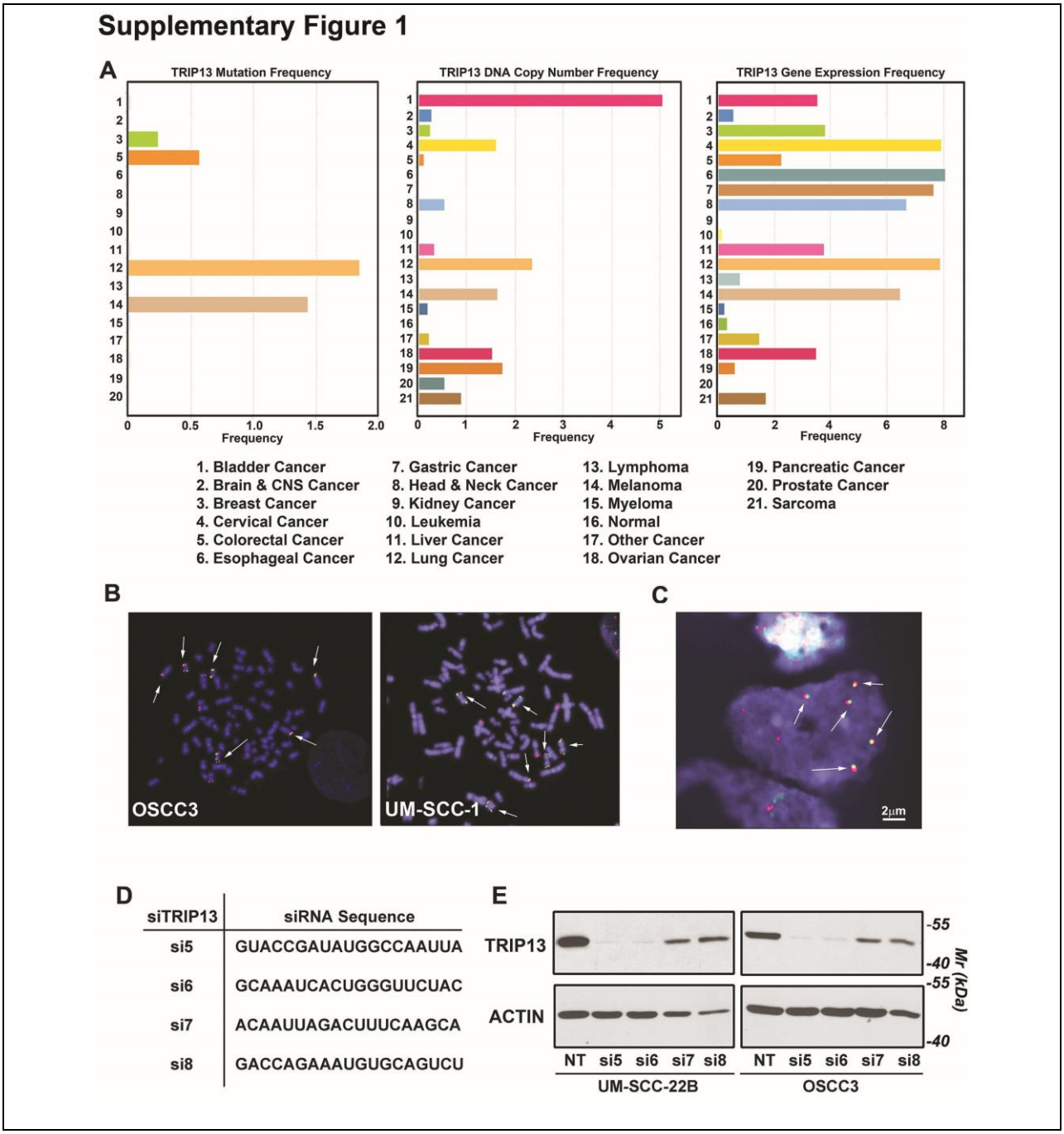

Supplementary Figure 1: *TRIP13* is amplified and overexpressed. A) Meta-analysis of *TRIP13* mutation, DNA copy number and gene expression in multiple cancers using Oncomine. **B)** Fluorescent in situ hybridization (FISH) shows an increase in *TRIP13* copy number in OSCC3 and UM-SCC-1, SCCHN cell lines. **C)** FISH on a human SCCHN shows amplification of *TRIP13* copy number relative to normal adjacent tissue (bar=2μm). **D)** Four siRNAs targeting TRIP13 were analyzed for effectiveness in downregulation of TRIP13. **E)** Lysates from UM-SCC-22B and OSCC3 transfected with siTRIP13 were immunoblotted with TRIP13 and actin antibodies

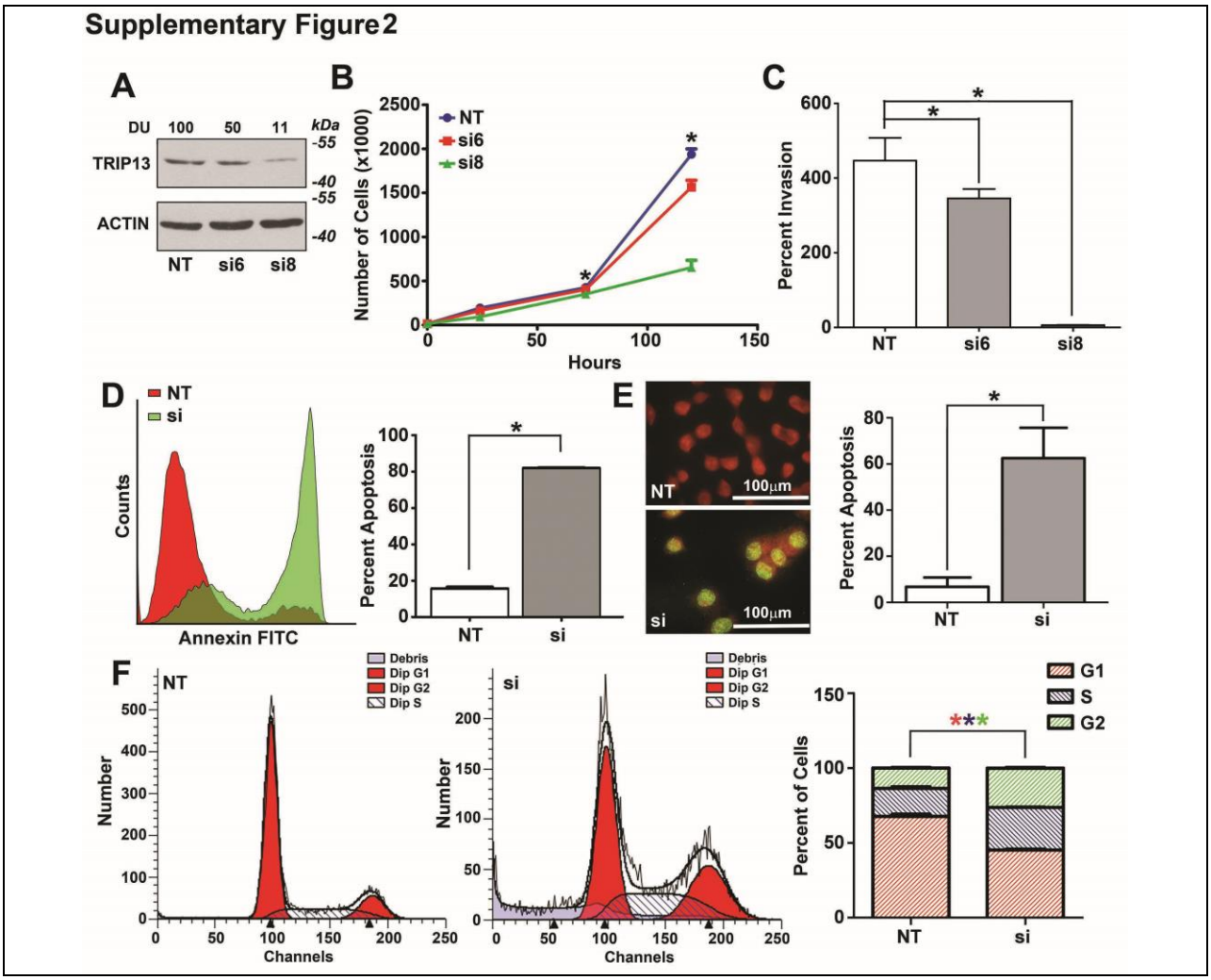

Supplementary Figure 2: Suppression of TRIP13 inhibits oncogenic phenotypes in OSCC3. OSCC3 cells were transfected with two different siRNAs for TRIP13 (si6,si8) or NonTarget (NT) siRNA. **A)** Cell lysates were immunoblotted with antibodies to TRIP13 and actin as a loading control. Signal intensity was quantified, normalized to actin and expressed as percent of NT. **B)** Cells were counted on days 1, 3 and 5 after seeding. Data are representative of three independent experiments with three replicates in each experiment. (Student's t-test with SEM, $p<0.02$) **C)** Cells were seeded equally on matrigel coated inserts. Invasion was measured 48hrs after seeding. Data are representative of three independent experiments with three replicates in each experiment (Student's t-test with SEM, $p<0.04$) **D)** Cells were seeded equally and apoptosis was measured by staining with FITC-AnnexinV and propidium iodide and were analyzed with flow cytometry. Data are representative of two independent experiments with three replicates in each experiment (Student's t-test with SEM $p<0.003$). **E)** Cells were seeded equally on poly-L-lysine coated coverslips and the TUNEL assay was performed to visualize apoptotic cells (green), which were quantified (bar=100μm). **F)** Cells were seeded equally and synchronized. Cell cycle analysis was performed by flow cytometry. Data are representative of two independent experiments with three replicates in each experiment (Student's t-test with SEM, $p<0.05$).

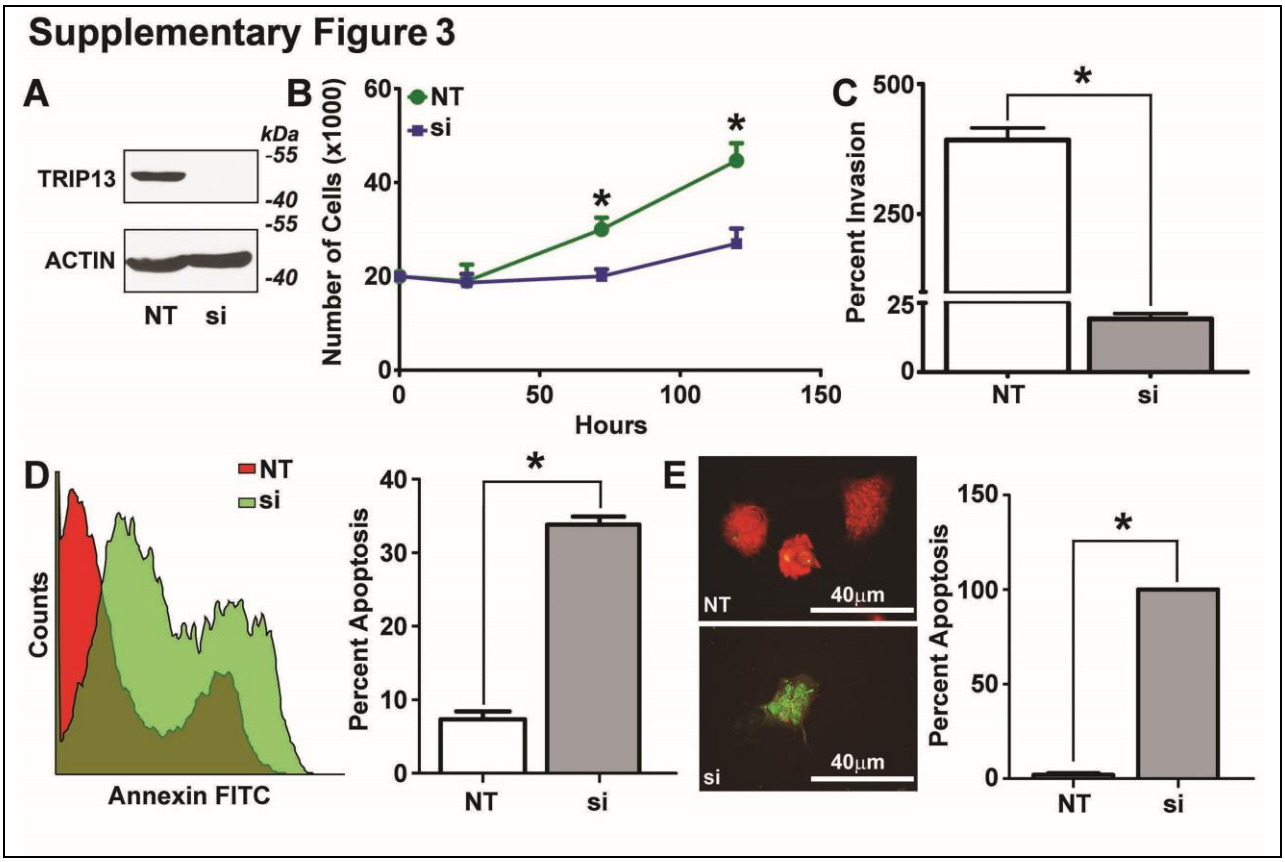

Supplementary Figure 3: Suppression of TRIP13 inhibits oncogenic phenotypes in UM-SCC-5. UM-SCC-5 cells were transfected with si8 for TRIP13 or NT-siRNA. **A)** Lysates were immunoblotted with antibodies to TRIP13 and actin as a loading control. Signal intensity was quantified, normalized to actin and expressed as percent of NT. **B)** Cells were counted on days 1, 3 and 5 after seeding. Data are representative of three independent experiments with three replicates in each experiment (Student's t-test with SEM $p<0.03$). **C)** Cells were seeded equally on matrigel coated inserts. Invasion was measured 48hrs after seeding. Data are representative of three independent experiments with three replicates in each experiment. **D)** Cells were seeded equally and apoptosis was measured using flow cytometry. Data are representative of two independent experiments with three replicates in each experiment (Student's t-test with SEM $p<0.03$). **E)** Cells were seeded equally on poly-L-lysine coated coverslips and the TUNEL assay was performed to visualize apoptotic cells (green), which were quantified (bar=40μm) (Student's t-test with SEM, *$p<0.03$).

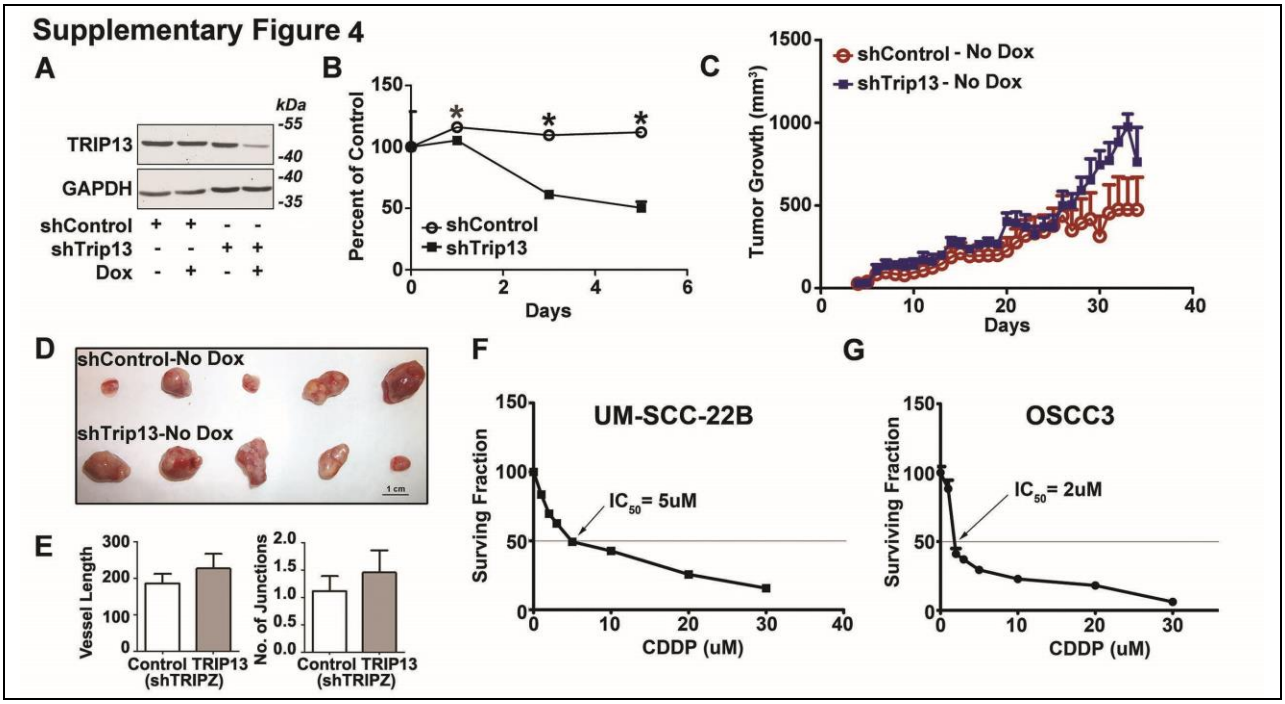

Supplementary Figure 4: Inducible suppression of TRIP13. **A)** OSCC3 cells were stably transfected with inducible-shTRIP13 or shControl and lysates from doxycycline-induced and non-induced cells were immunoblotted with TRIP13 and GAPDH antibodies. **B)** OSCC3-shControl and -shTRIP13 cells were seeded, induced and counted. Data represent three independent experiments with three replicates in each experiment (Student's t-test with SEM, $p<0.03$). **C and D)** UM-SCC-22B-shControl and -shTRIP13 cells were injected subcutaneously into mice. (These are no-induction controls for Figure 3C and 3D). **C)** Tumors were measured daily for 34d and tumor volume was calculated. **D)** Gross appearance of tumors; shControl (upper) and shTRIP13 (lower) (bar=1cm). **E)** Doxycycline inducible UM-SCC-22B-shControl and -shTRIP13 cells ($1X10^6$) were seeded on CAM for tumor growth and angiogenesis was quantified from the tissue sections. **F and G)** IC50s of CDDP for UM-SCC-22B (**F)** and OSCC3 (**G)** were determined by seeding cells equally and treating with the indicated doses of CDDP for 2hrs. 72hrs later, cells were counted and percent survival was calculated. Data are representative of three independent experiments with three replicates in each experiment.

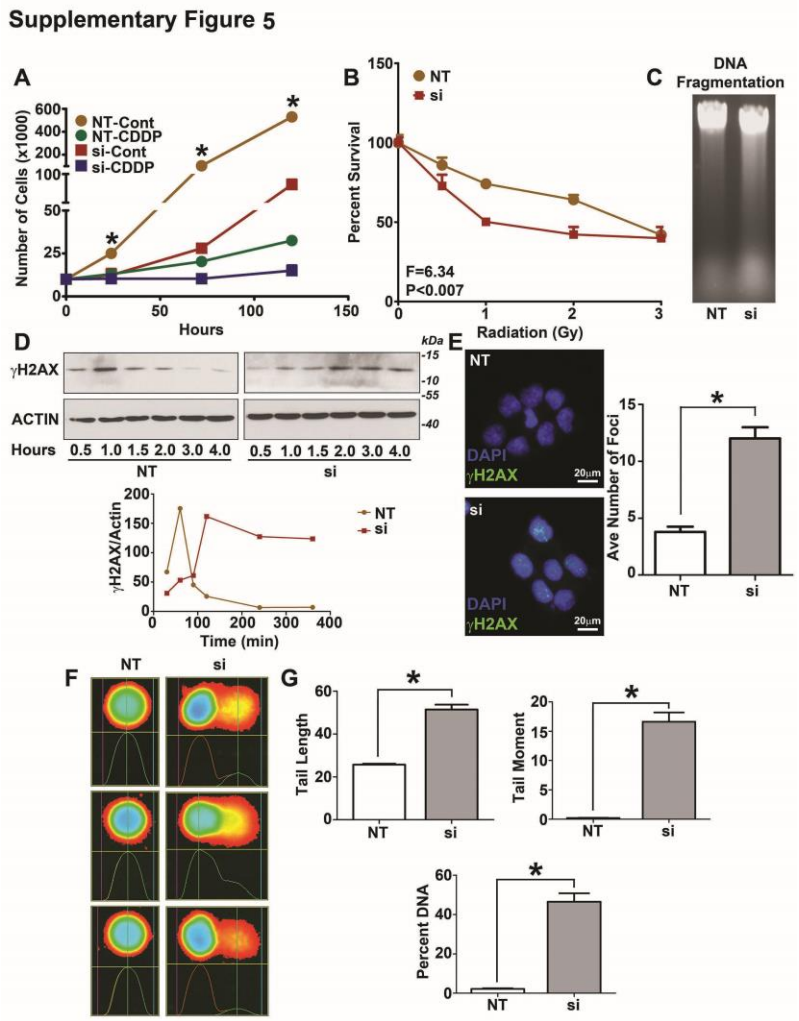

Supplementary Figure 5: Suppression of TRIP13 increases DNA damage in OSCC3. OSCC3 cells were transfected with siTRIP13 or si NonTarget. **(A)** Cells were seeded equally, treated with 2uM CDDP for 2hrs and then counted on days 1, 3 and 5 after seeding. Data are representative of three independent experiments with three replicates in each experiment. **(B)** Cells transfected with NT (~1,000) or siTRIP13 (~10,000) were irradiated at 0.5, 1, 2 and 3 Gy five days after plating. After an additional 7-14 days, colonies were fixed, stained with crystal violet and counted. Data are representative of three independent experiments with three replicates in each experiment (Student's t-test with SEM, p<.01). **(C)** Cells were synchronized with nocodozole and irradiated at 2Gy. Genomic DNA was isolated, electrophoresed, and visualized with ethidium bromide. **(D)** Cells were irradiated at 2Gy and lysates were collected at 30min, 60min, 90min, 2hrs, 3hrs and 4hrs later. Whole cell lysates were immunoblotted with γH2AX and actin as a loading control. Signal intensity was quantified and plotted over time (bottom graph). **(E)** Cells were seeded on poly-L-lysine coated coverslips and immunoflourescence was performed with γH2AX antibody. The average number of γH2AX foci (green) per cell was calculated for NT and siTRIP13 (bar=20μm). **(F)** Comet assay of NT and siTRIP13 cells shows DNA damage within the cells. **(G)** Tail length, tail moment, and percent DNA in the tail were calculated for NT and siTRIP13 cells (Student's t-test with SEM, p<0.04).

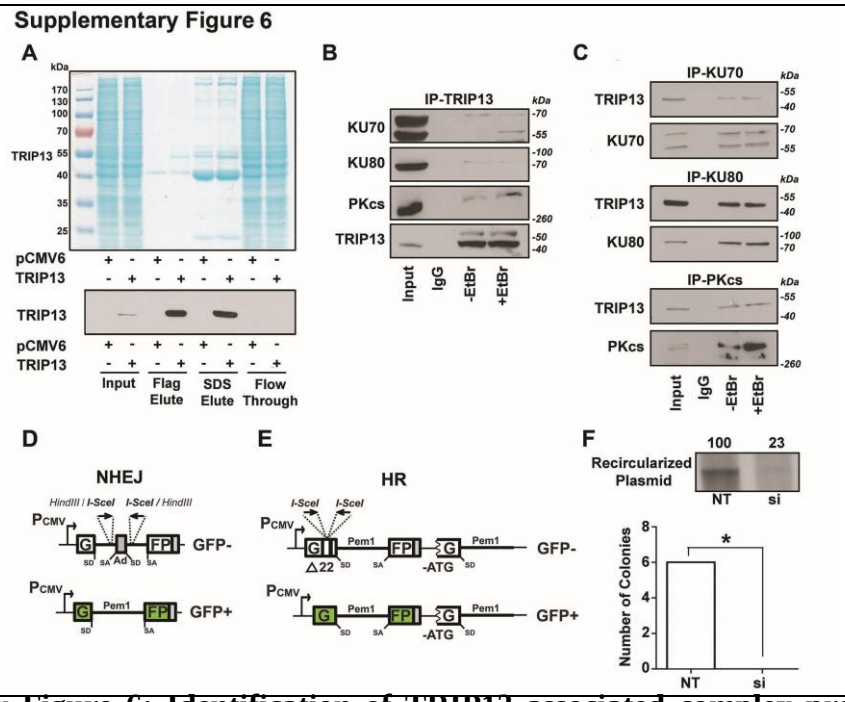

Supplementary Figure 6: Identification of TRIP13 associated complex proteins by mass spectrometry. (A) Flag-tagged TRIP13 and its co-complex proteins were purified from UM-SCC-1-TRIP13-Flag and UM-SCC-1-Flag cells. After elution of recombinant protein with FLAG-peptide, elution efficiency of purified protein was verified by Coomassie-stained gel (top) and immunoblot (bottom). The purified protein was used for mass spectrometry. **(B)** Endogenous TRIP13 from OSCC3 was immunoprecipitated in the presence or absence of ethidium bromide and immunoblotted with KU70, KU80, PKcs and TRIP13 antibodies. **(C)** KU70, KU80 and DNA-PKcs were immunoprecipitated in the presence or absence of ethidium bromide and immunoblotted with anti-TRIP13. **(D and E)** Schematics of the NHEJ and HR reporter constructs used in this study. Adapted from [1]. **(D)** In the NHEJ repair reporter construct, the GFP gene is interrupted by an adenoviral exon sequence (Ad) and GFP is not expressed. Concurrent transfection with the I-SceI endonuclease expression plasmid induces DSBs by excising the exon at the flanking recognition sequences for the I-SceI endonuclease. This DSB, when repaired by NHEJ can only result in GFP expression. **(E)** The I-SceI endonuclease plasmid when transiently co-transfected with the HR reporter construct generates a DSB in the GFP reporter construct. The GFP cassette of the HR reporter construct has a deletion in the first exon adjacent to an insertion with I-SceI/HindIII/I-SceI sites. The two I-SceI sites are in inverted orientation and have incompatible cut ends. A second GFP gene without a promoter or start site and missing the second exon is downstream of the GFP reporter gene. DSB repair can only occur by HR between the truncated exon on the first cassette and the first exon of the second GFP gene [1]. Due to the deletion in the first exon, NHEJ cannot restore GFP expression. **(F)** A mini-NHEJ extract from OSCC3 cells transfected with NT or siTRIP13 was incubated with linear plasmid with non-cohesive ends. The end joining product was purified and the recircularized plasmid was visualized on agarose gel stained with ethidium-bromide. An aliquot of recirculaized plasmid was used to transform bacteria and colonies were counted (bottom graph) (Student's t-test with SEM, $p<0.005$).

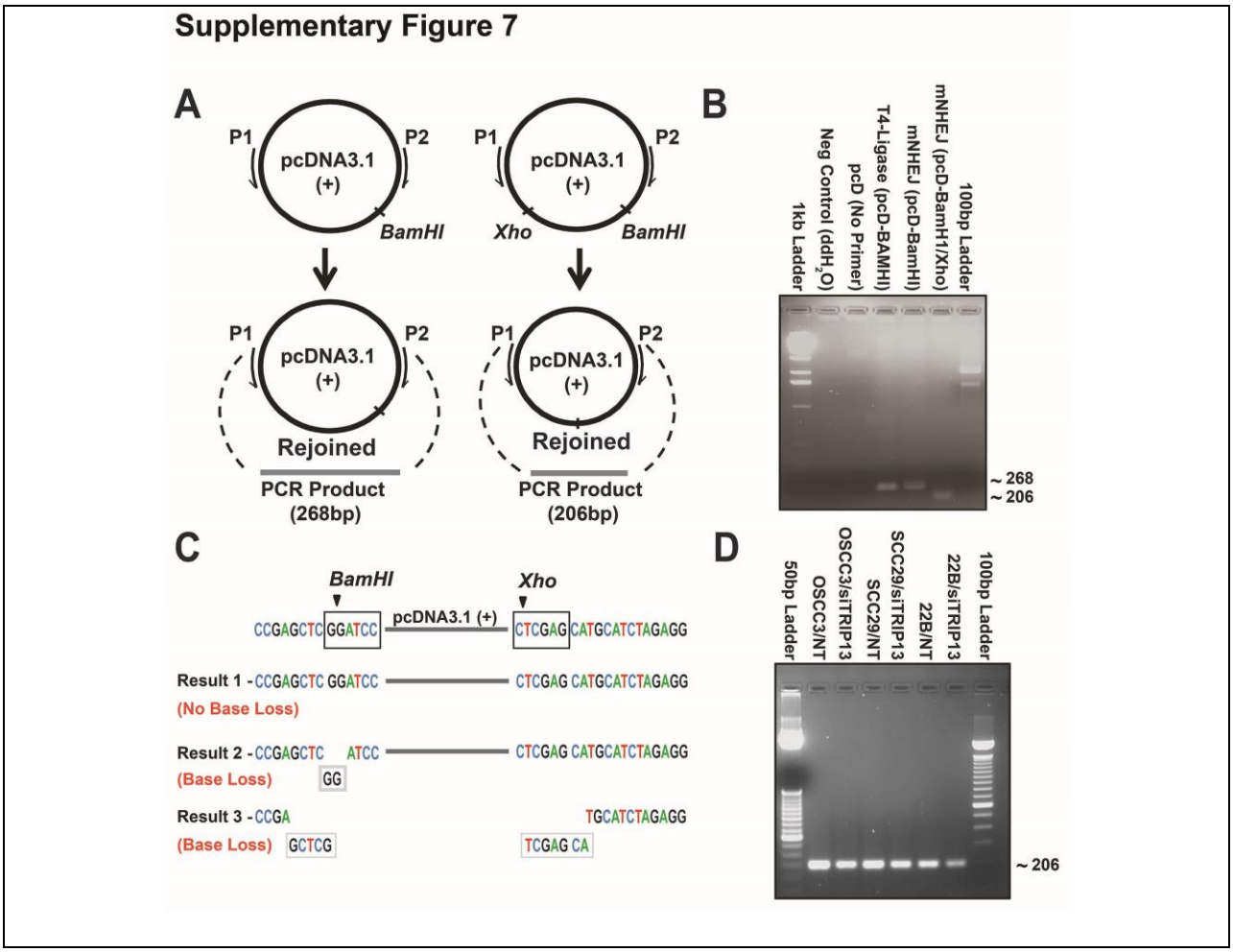

Supplementary Figure 7: TRIP13 promotes NHEJ repair. A) Schematic to show the variation in size of PCR products with NHEJ repair for singly digested or doubly digested plasmid vector used for the optimization of mini-NHEJ assay. **B)** pcDNA 3.1 was digested with restriction endonuclease indicated in the figure singly or doubly to make linear fragments that were rejoined with mini-NHEJ extracts prepared from UM-SCC-22B cells. The rejoined product was transformed into bacteria and the plasmid was purified from representative colonies that were linearized with BamHI and ligated with T4 ligase (lane 4), linearized with BamHI and rejoined with mini-NHEJ extract (lane 5), BamHI and XhoI double digested and rejoined with mini-NHEJ extract (lane 5). A standard PCR was performed with these plasmids with primers listed in Supplementary Table 4. Corresponding product size is indicated in the figure that confirms the real rejoining. **C)** Purified plasmids from the rejoined mini-NHEJ product (after bacterial transformation) were further sequenced to confirm NHEJ. Random base loss was observed near the DSB repair region for both single and double digested rejoined product. Representative sequence shown from sequence with maximum base loss. **D)** *In-vitro* NHEJ repair reaction was performed with BamHI/XhoI double-digested pcDNA3.1 vector and with mini-NHEJ extracts prepared from cells treated with NT and siTRIP13 in different SCCHN cell lines. A semi-quantitative PCR reaction for 15 cycles was performed and run on an agarose gel and stained with ethidium bromide prior to image capture.

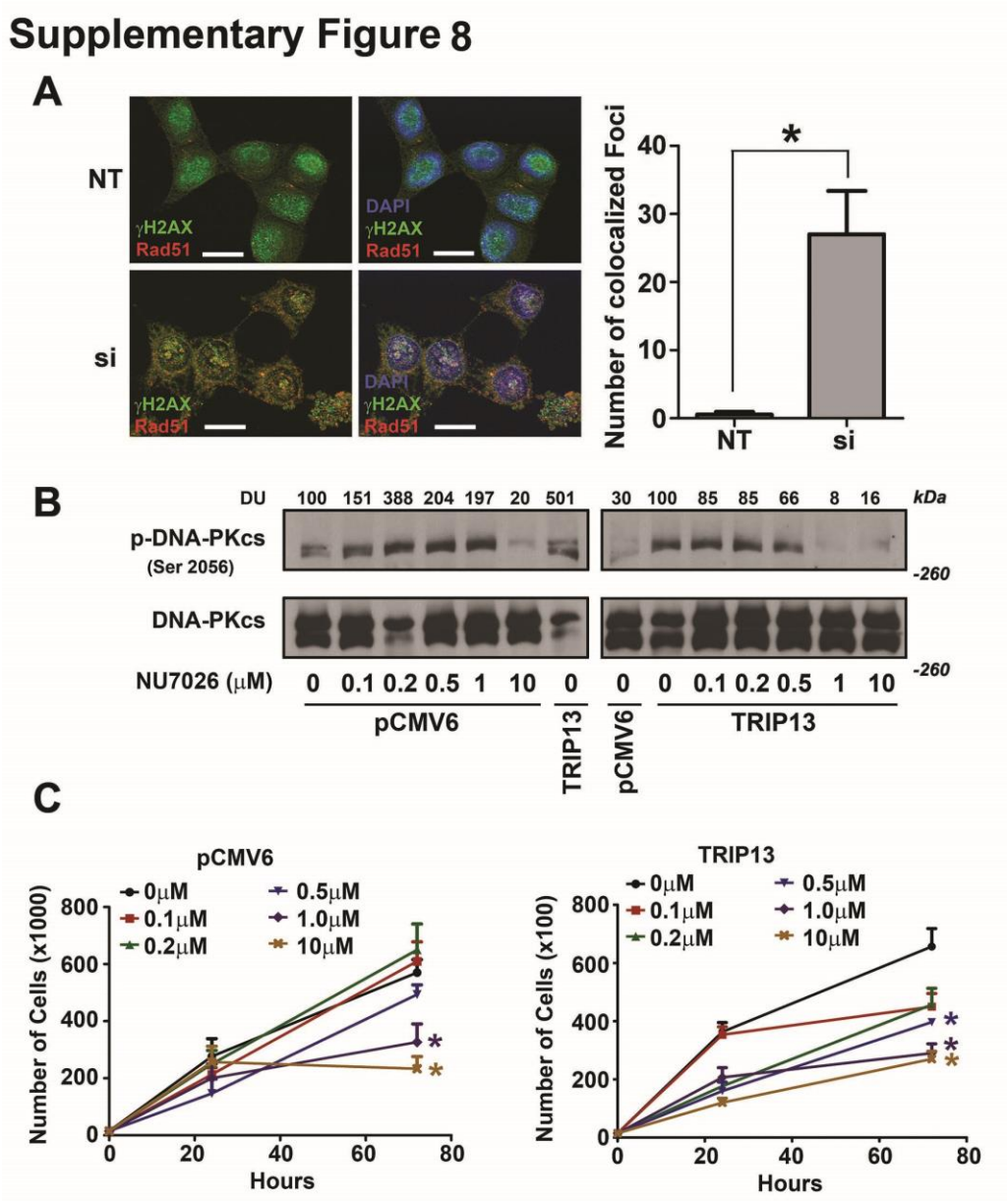

Supplementary Figure 8. TRIP13 expression is inversely correlated with RAD51/γH2AX co-localization; and Effect of Nu7026 on DNA-PKcs autophosphorylation and proliferation. A) OSCC3 cells transfected with NT or siTRIP13 were seeded on poly-L-lysine coated coverslips. Cells were stained with γH2AX (green) and Rad51 (red) antibodies as well as DAPI (blue) (bar=20μm). Rad51 and γH2AX co-localized foci (orange) were counted and graphed (Student's t-test with SEM $p<0.005$). **B)** UM-SCC-1 cells overexpressing TRIP13 or control vector pCMV6 were treated with increasing concentrations of NU7026 for 72h and were immunoblotted with phospho-DNA-PKcs (Ser2056) and DNA-PKcs antibodies and were quantified. **C)** Cells overexpressing TRIP13 or control pCMV6 empty vector were treated with different concentrations of NU7026, counted on days 1, 3 and 5, and graphed (Student's t-test with SEM, $p<0.03$). Data are representative of 3 independent experiments with 3 replicates in each experiment.

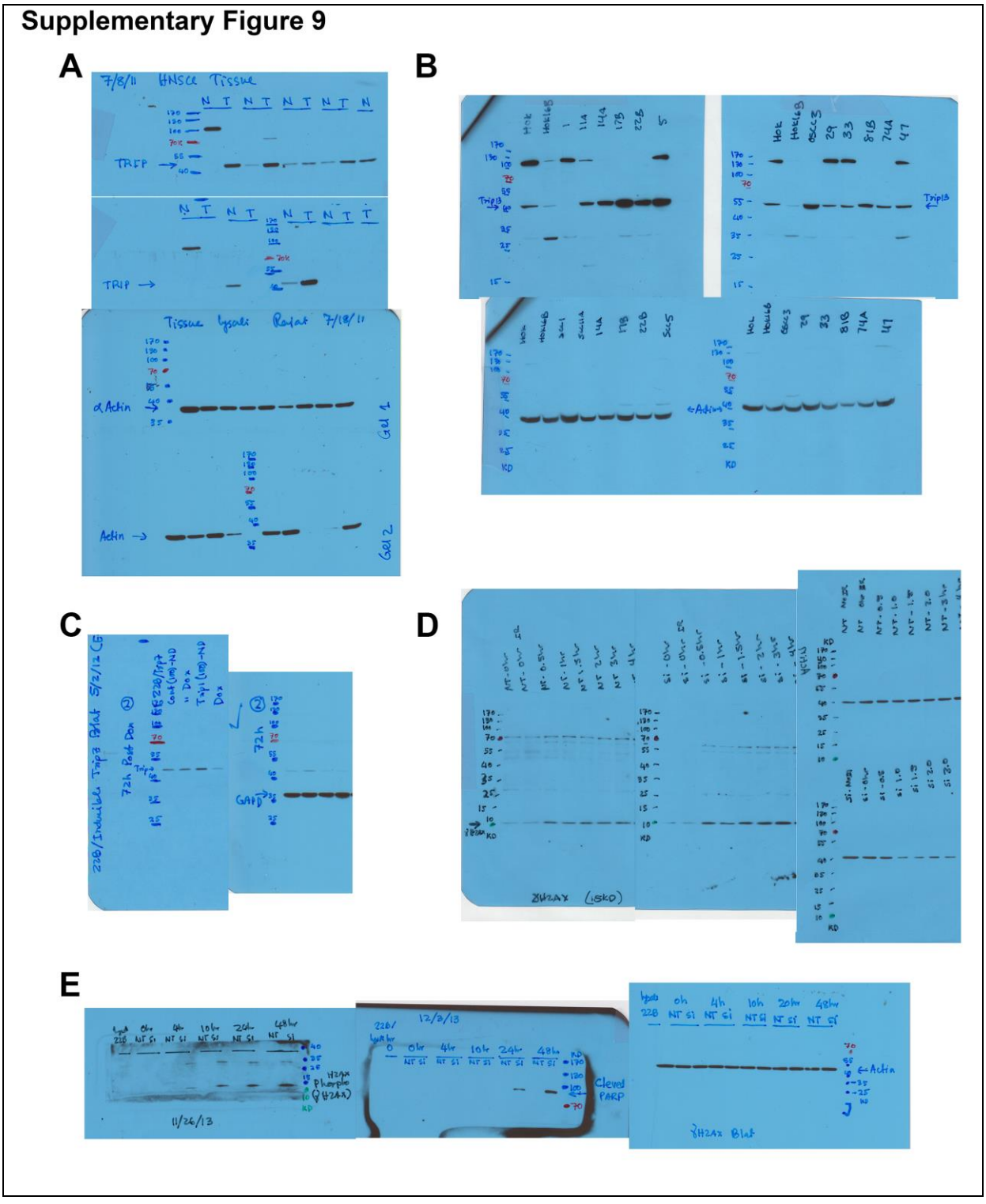

Supplementary Figure 9. Uncropped scans of immunoblots used for: A) Figure 1D; **B)** Figure 2B; **C)** Figure 3A; **D)** Figure 5D; and **E)** Figure 5H.

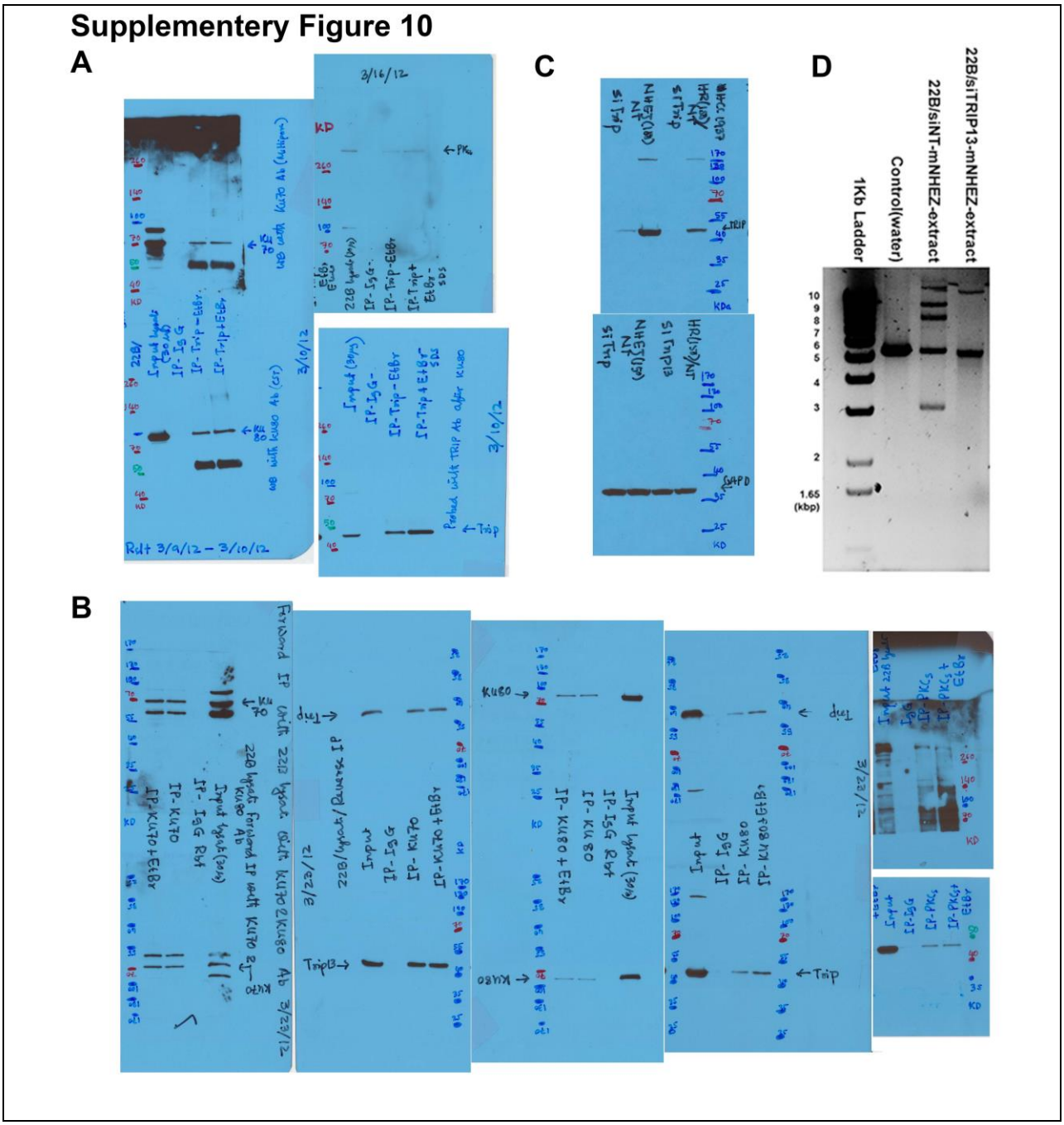

Supplementary Figure 10. Uncropped scans of immunoblots used for: A) IP with TRIP13 antibody used for Figure 6C; **B)** IP with KU70, KU80 and DNA-PKcs antibodies used for Figure 6D; **C)** TRIP13 knockdown with siTRIP13 in HCC1937 cells stably overexpressing HR and NHEJ constructs used for flow cytometry for HR/NHEJ efficiency in Figure 6E, 6G; **D)** Agarose gel run for mini-NHEJ assay for re-circularized plasmid used for Figure 6F.

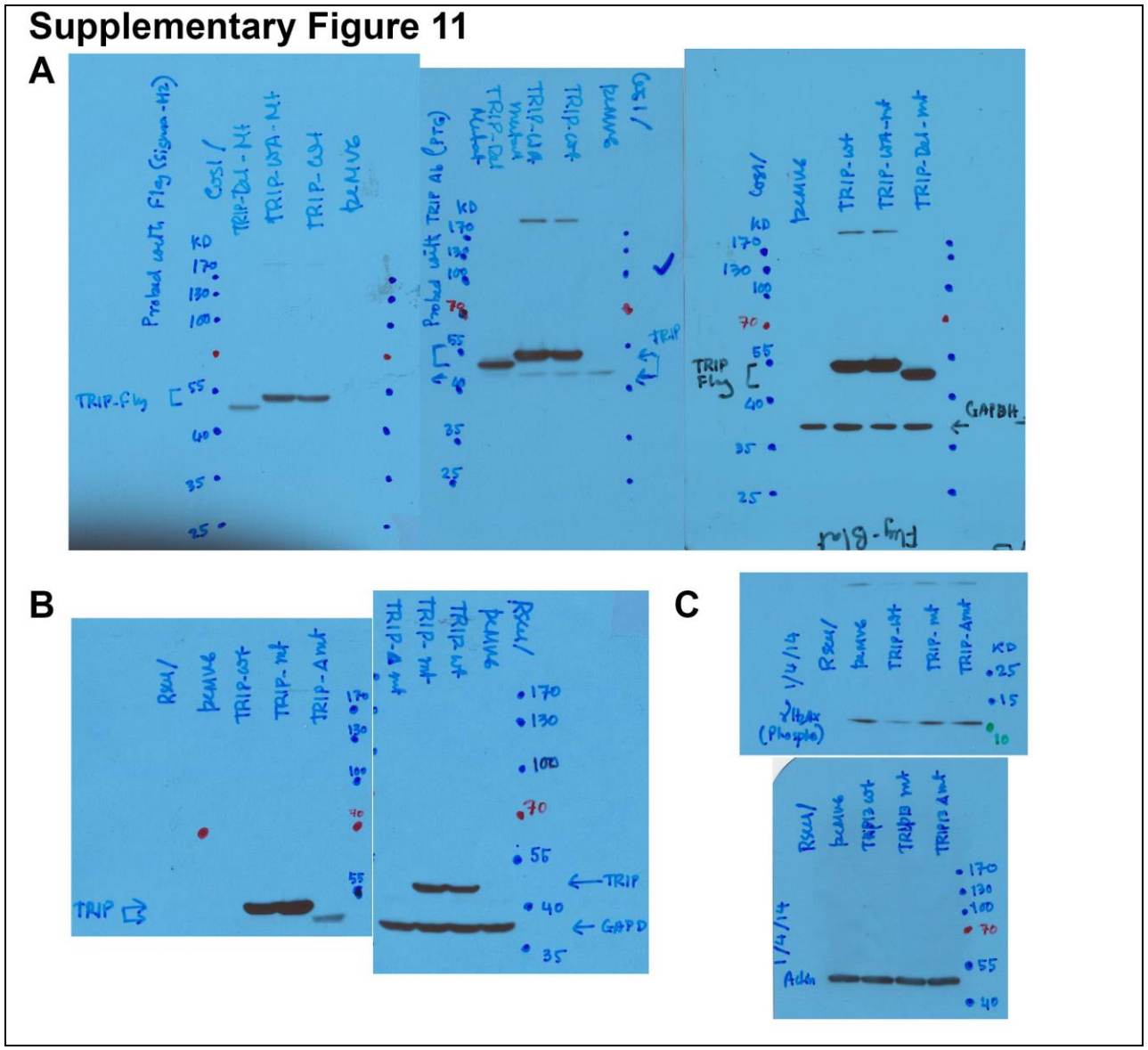

Supplementary Figure 11. Uncropped scans of immunoblots used for: A) Expression of TRIP13 and TRIP13-mutant constructs transfected in COS-1 cells, used for Figure 8B; **B)** Expression of TRIP13 and TRIP13-mutant constructs stably transfected in UM-SCC-1 cells used for Figure 8E; **C)** γH2AX blot used for Figure 8H.

SUPPLEMENTARY TABLES

Supplementary Table 1

Clinical Data of Specimens		
Gender		
	Male	40
	Female	20
Age		
	< 50 years	13
	50 - 70 years	41
	> 70 years	6
TNM Staging		
	Stage I	25
	Stage II	16
	Stage III	7
	Stage IV	10
Tumor Grade		
	Well Differentiated	45
	Moderately Differentiated	9
	Poorly Differentiated	2
	Undifferentiated	0

Supplementary Table 1. Clinical data and tumor information linked to SCCHN specimens represented on the tissue microarray (TMA). Information is presented according to age, and tumor stage and grade.

Supplementary Table 2

Protein ID	Protein probablity	Unique Peptides	% Coverage	Total Peptides	Description
Q15645	1	46	64.8	1166	TRP13 HUMAN Thyroid receptor-interacting protein 13
Q9P0V0	1	115	46.9	269	SPTA2 HUMAN Spectrin alpha chain, brain
P05023	1	22	27.9	92	AT1A1 HUMAN Na/K-transporting ATPase subunit alpha-1
P12956	1	15	30.7	28	XRCC6 HUMAN X-ray repair cross-complementing protein 6 (KU70)
P60953	1	4	25.4	24	CDC42 HUMAN Cell division control protein 42 homolog
P80723	1	8	33.1	20	BASP1 HUMAN Brain acid soluble protein 1
B4DWW4	1	10	43.7	18	B4DWW4/MCM3 HUMAN Minichromosome maintenance deficient 3 (S. cerevisiae), isoform CRA_b
P04908	1	3	42.5	16	H2A1B HUMAN Histone H2A type 1-B/E
Q9UDL5	1	9	16.8	15	STAT1 HUMAN Signal transducer and activator of transcription 1-α/β
Q14683	1	10	9.7	14	SMC1A HUMAN Structural maintenance of chromosomes protein 1A
E7BSV0	1	6	28.2	14	EGFR HUMAN Epidermal growth factor receptor variant A
Q6FHF5	1	5	19.2	12	PCNA HUMAN Proliferating cell nuclear antigen
P09874	1	7	9.1	10	PARP1 HUMAN Poly [ADP-ribose] polymerase 1
P13010	1	6	8.9	10	XRCC5 HUMAN X-ray repair cross-complementing protein 5 (KU80)
Q9NTJ3	1	6	5.9	10	SMC4 HUMAN Structural maintenance of chromosomes protein 4
Q9Y265	1	6	17.5	8	RUVB1 HUMAN RuvB-like 1
Q71UI9	1	3	31.2	7	H2AV HUMAN Histone H2A.V
Q9UME3	1	4	1.3	7	PRKDC HUMAN DNA-dependent protein kinase catalytic subunit
Q16531	1	5	8.2	7	DDB1 HUMAN DNA damage-binding protein 1
Q75M87	1	5	6.8	6	GTF2I HUMAN General transcription factor II-I
B4DM41	1	3	9.9	5	RFC4/B4DM41 HUMAN Replication factor C (Activator 1) 4, 37kDa, isoform CRA_b
Q9UQE7	1	3	3.9	5	SMC3 HUMAN Structural maintenance of chromosomes protein 3
P06493	1	2	7.7	4	CDK1 HUMAN Cyclin-dependent kinase 1
O95347	1	2	1.8	3	SMC2 HUMAN Structural maintenance of chromosomes protein 2
O60216	1	2	4.8	2	RAD21 HUMAN Double-strand-break repair protein rad21 homolog
Q09028	1	2	5.9	2	RBBP4 HUMAN Histone-binding protein RBBP4
Q5T0Y4	1	1	13.7	1	MDM4 HUMAN Mdm4 p53 binding protein homolog (Mouse)
P27695	1	1	11.9	1	APEX1 HUMAN DNA-(apurinic or apyrimidinic site) lyase, mitochondrial

Supplementary Table 2. List of TRIP13 interacting proteins identified by LC-MS/MS mass spectrometry: List of highest probabilistic proteins interacting with TRIP13 as identified by LC-MS/MS mass spectrometry. Summary of proteins with protein probability 1 and their features is listed. From the filtered protein list common contaminant, keratins, and decoy proteins were removed manually to generate a short list for TRIP13 interacting proteins.

Supplementary Table 3

Term	p-value
Non-Homologous End-Joining	**0.0007**
Cell Cycle	**0.0007**
Base Excision Repair	**0.0047**
Mismatch Repair	0.0717
DNA Replication	0.1400
Nucleotide Excision Repair	0.2140
Oocyte Meiosis	0.8460
Basal Transcription Factors	1.0000
Systemic Lupus Erythematosus	1.0000
p53 Signaling Pathway	1.0000
Wnt Signaling Pathway	1.0000

Supplementary Table 3. Significance associated with Kegg Pathways: The short listed TRIP13 interacting proteins were submitted to the string database (http://string-db.org/) to visualize a molecular network and associated significance in the Kegg pathway.

Supplementary Table 4

Primer Name	Primer Sequence
TRIP13GE-FP	5'-CTG GAG GAA GAG ACA GAA AAC ATA A-3'
TRIP13GE-RP	5'-GTT GTC ATC ACA TAA TCG AGG AGA T-3'
P1 Forward	5'-TAA CTA GAG AAC CCA CTG CTT ACT-3'
P1 Reverse	5'-CTT CCA GGG TCA AGG AAG GCA CG-3'
TRIP13FullCloneOriFP	5'-ATA AGC AGA GCT CGT TTA GTG AAC CGT CAG AAT-3'
TRIP13FullCloneOriRP	5'-GAG GCG GAG ATT GCA GTG AGC CAA GAT TG-3'
TRIP13WALKERAG184ASe	5'-ACG GTC CTC CTG GCA CTG CAA AAA CAT CCC TGT GT-3'
TRIP13WALKERAG184AAs	5'-ACA CAG GGA TGT TTT TGC AGT GCC AGG AGG ACC GT-3'
TRIP13AAADelFP	5'-ATT AAA AGG CAT TCC AAT GCT GAC ATC AAG CAG TAC-3'
TRIP13AAADelRP	5'-GTA CTG CTT GAT GTC AGC ATT GGA ATG CCT TTT AAT-3'

Supplementary Table 4. List of primers used to quantify TRIP13 expression, verify rejoined plasmid DNA and generate TRIP13 mutants: List of primers used to quantify TRIP13 expression in cell lines; amplify PCR product to verify rejoining mediated by mini-NHEJ extracts of pCDNA3.1(+) vector digested with BamHI or double digested with BamHI-XhoI; and primers used for making TRIP13 WalkerA motif point and TRIP13 deletion mutants.

SUPPLEMENTARY METHODS

Angiogenesis analysis

Inducible UM-SCC-22B-TRIPZ-shControl and -shTRIP13 cells ($1x10^6$) were seeded on the CAM,of a 10 day old chicken embryo, an *in-vivo* model of angiogenesis in SCCHN. Upper CAM was excised after day 14, fixed and photographed for fluorescently labelled cells and for the vasculature. AngioTool (https://ccrod.cancer.gov/confluence/display/ROB2/Home) was used to quantify the vasculature.